IEEE Access
Multidisciplinary | Rapid Review | Open Access Journal

Received June 19, 2018, accepted July 24, 2018, date of publication August 1, 2018, date of current version August 28, 2018.

Digital Object Identifier 10.1109/ACCESS.2018.2861915

Tractable Mobility Model for Multi-Connectivity in 5G User-Centric Ultra-Dense Networks

HONGTAO ZHANG, (Senior Member, IEEE), AND WANQING HUANG, (Student Member, IEEE)
School of Information and Communication Engineering, Beijing University of Posts and Telecommunications, Beijing 100876, China

Corresponding author: Hongtao Zhang (htzhang@bupt.edu.cn)

This work was supported by the National Science Foundation of China under Grant 61302090.

ABSTRACT With the network densification, frequent handovers may degrade mobility reliability, cause heavy signaling load thus blocking the improvement of network capacity. This paper aims at reducing cost in terms of handover in dense networks, deriving compact expressions of network performance metric, including handover probabilities as well as the mobility-aware downlink data rate, under a multi-connectivity mobility model in user-centric ultra-dense networks (UUDNs). Specifically, the nearest M access points (APs) in mobile user's vicinity serve the user for data transmission, while the best one among them is for control, which reduces handover probability and network overheads without a loss in the throughput performance gain. Based on the scheme, handover probabilities are derived for arbitrary movement trajectory in the UUDN, where the locations of APs are modeled as a homogeneous Poisson point process, and then is included in handover cost to derive the downlink rate for mobile users. It is shown that the handover probability in control-plane can considerably be decreased by at least 30% compared with the traditional single connectivity network. What is more, the downlink rate can be improved significantly by 2× compared with single connectivity.

INDEX TERMS User-centric ultra-dense network, multi-connectivity, handover, Poisson point process.

I. INTRODUCTION

The impetuous increases in the amount of mobile users and their traffic demands push cellular network operators to provide a higher-capacity network [1]. As one of the emerging techniques in the fifth generation (5G), ultra-dense networks (UDN) provide higher network capacity by shrinking the service distance [2], [3]. However, the network densification means stronger inter-cell interference and higher handover rate, which would bring higher network control overheads and, consequently, higher handover failure rate [4].

In order to mine the potentials of UDN, the network architecture is transformed from traditional cell-centric to user-centric [5]. The philosophy of user-centric ultra-dense networks (UUDN) is introduced by changing from a network controlling user to a network serving user [6]. UUDN will organize a dynamic access point group (APG) and flexibly allocate the required resource to provide satisfactory services along with each user's movement [7].

The dynamic APG forming can be realized by multi-connectivity which strongly provides user-centric services [8]. On the one hand, multi-connectivity can bring higher throughput [9]. The average per user throughput is improved since having extra traffic links will obviously add diversity gain [10], and overcome the backhaul limitation of single connectivity [11]. On the other hand, multi-connectivity improves the mobility robustness, considerably decreasing the number of handover failures [8], [12]. The handover rate is reduced by expanding the coverage area of the serving cells [7] and the continuous services can be enjoyed even when changing the set of serving access points (APs) [13]. Attracted by its advantages, multi-connectivity scheme is designed to improve handover [15] and the link blockage performance [14] for millimetre wave (mmWave) cellular network.

The gain brought by multi-connectivity comes at the expense of more signal overheads due to the frequent forming/reforming of APG [16]. In order to lessen the network control overheads and reduce handover delay, control-plane and user-plane (CP/UP) split network architecture is introduced [17]. Under this architecture, only the cell specific control signals for the specific APs are broadcast, and this specific AP manages handover events of other APs without informing the core network [7].

It would be useful to generalize the results of multi-connectivity in UUDN, for the purpose of enhancing user mobility and reducing handover rate at the same time, which,

however, has not been explored in existing literatures. Therefore, a tractable model for multi-connectivity should be investigated, including analyses of the handover rate and downlink rate.

A. RELATED WORKS

In order to characterize the handover rate without loss of the spatial randomness, homogeneous Poisson point process (PPP) model is widely used for its tractability and applicability [18]–[23]. The fundamentals of mobility are introduced in [18]. To best our knowledge, state of the art studies of handover performance mostly focus on dense multi-tier heterogeneous networks (HetNet), where a bias factor is introduced to maximize the coverage of small cells [19]–[21]. Further, the vertical and horizontal handover rates are calculated in [22] by normalizing the transmission power and range extension bias in different tier. Moreover, [23] takes the effect of small scale fading into consideration, compared handover rate with and without perfect channel state information (CSI).

Different from the aforementioned models, few stochastic geometric models for mobility performance with multi-connectivity can be found. In [17], the mobility-aware average throughput with CP/UP split architecture is calculated where a user can connect with a macro cell and a small cell, but only one cell serves the user in user-plane. To maintain connections from one user to multiple APs, the handover rate in user-centric cooperative networks is derived in [24]. Based on [24] and [16] quantifies the tradeoff between the handover rate and the data rate for multiple association without specific transmission scheme, so that the model is applicable to many different scenarios. However, the works in [17] and [16] have some imperfections:

- The clusters of the serving cells in [17] are designed in a cell-centric approach, where the edge user is served by a small cell and a macro cell at different time. In this paper, a user-centric APG is formed to improve the system throughput as well as mobility robustness by remaining multiple connections simultaneously. Thus the handover is related to the irregular region of the user-centric APG, where the mobility model involves changes of a set of serving APs.
- The number of handovers for multiple association is quantified in [16] where the update of AP clusters is managed through mobility management entity (MME), causing more control overheads due to the larger cluster size. However, in this paper, an anchor AP is chosen for managing the forming/reforming of the AP clusters to enable the transparent handover to the MME. Therefore, compared to the static network topology in [16], the boundaries of AP clusters change dynamically according to the locations of the anchor APs.
- The data rate is characterized in [16] and is further included in the tradeoff together with the handover rate to optimize the cluster size by defining the utility values. However, the optimal cluster size depends on the utility values, where direct mapping function with network factors (e.g. signaling overheads and handover failure rate) cannot be found. On the contrary, the handover cost in this paper is the function of the handover rate and handover delay which is determined by the network.

B. CONTRIBUTIONS

Different from the aforementioned lectures, our proposed multi-connectivity model aims to enhance the mobility performance by expanding coverage area of APGs that serve users. To the best of our knowledge, the multi-connectivity performance on user mobility in homogeneous small cells UUDN environment has not yet been investigated. It is assumed that the number of APs is much larger than the number of users, so the network has abundant radio resource to serve the user with required high data rate by multi-connectivity. Handover probabilities are derived, and objectively included in handover cost to compute the downlink rate. Referencing to [20], the handover probability is defined as the probability that the handover occurs in a unit time. The main contributions of this paper are as follows:

- User-centric APG is formed with multi-connectivity to benefit from both joint transmission and mobility robustness. The dynamic APG is updated through user's movement, ensuring that user is always in the center of the transmission group. Moreover, an anchor AP which manages the dynamic APG update procedure is chosen to lessen handover signaling to the core network.
- The compact expressions of handover probabilities in both CP and UP are derived for multi-connectivity using stochastic geometry tools, which are closely related to the AP density, user velocity and the number of serving APs. The analysis of handover for multi-connectivity is more complicated compared to traditional single connectivity, since the locations of the anchor AP and the furthest serving AP after the movement are unknown.
- To state the significant impact of user mobility on data rate performance, the expression of mobility-aware average downlink rate of mobile users is then derived by including handover cost. The difference between handover delays in UP and CP as network parameters is taking into account, and the handover cost reflects the probability that user is experiencing a handover process.

II. SYSTEM MODEL

The network model and the multi-connectivity mobility model are described in this section. The key mathematical notations used in this paper are listed in Table 1.

A. NETWORK MODEL

One of the common two-dimensional (2D) spatial models with the advantage of analytical tractability is the PPP. This paper consider an irregular network, where APs and user equipments (UEs) are modeled as two independent 2D PPPs, respectively, to model spatial randomness. APs are

TABLE 1. Notation description.

Notation	Description
Φ_B, Φ_u	PPP of APs (or UEs)
λ_B, λ_u	Density of APs (or UEs)
$\Gamma_{u,k}$	Received signal power by UE u of k-th AP
P	Transmit power of APs
α	Path loss exponent
h_k	Multipath fading effect of the k-th AP
M	Active set size
$AP\ j$, $AP\ C$	The j-th nearest AP of UE; The control AP
l_1, l_2	Location of UE before (or after) UE moved
r_j, r_c	Distance between UE and the j-th AP (or control AP) before UE moved
R, R_c	Distance between UE and the j-th AP (or control AP) after UE moved
C, C_j, C_c	Circle with its center at l_1 and radius r_{M+1} (r_j or r_c)
A, A_c	Circle with its center at l_2 and radius R (or R_c)
v	Distance that UE moved in a unit of time
θ, θ_c	Angle with respect to the direction of the connection (or $AP\ C$)
H_u, H_c	Handover in user-plane (or control-plane)
F_j	Event that $AP\ j$ becomes the furthest serving AP after UE moved
N_{arc}, N^c_{arc}	Event that the arc of circle C included in A (or A_c) exclude $AP\ (M+1)$
S_I, S_{II}	$C_j \backslash C_j \cap A$, $(C \backslash A \cap C) \backslash S_I$
$\lvert S \rvert$	Measure of S
$N(\cdot)$	Number of APs in the specified area
$S_\cap(r, R, v)$	Common area between two intersecting circles with radius r and R, and the central distance v
C^n_M	Binomial Coefficient, $\frac{(M-1)!}{n!(M-n-1)!}$
$\bar{R}_j$	Average downlink rate with connection to the j-th AP
R^s_M, R_M	Total downlink rate of static users (or mobile users)
$\bar{d}_u, \bar{d}_c$	Delay incurred by handover in user plane (or control plane)
D	Handover cost
ASE	Area spectral efficiency

characterized as a PPP Φ_B with the tuple $\{P, \lambda_B\}$ denoting the transmit power and the AP density, respectively. UEs are characterized as a PPP Φ_u with its density λ_u. The nearest M APs in user's neighborhood form a dynamic APG to transmit data packets simultaneously for each user, termed as active set (AS). Moreover, M is the size of the AS.

In UUDN, there must be more handovers compared to traditional networks due to the densification of APs. Splitting CP and UP is proposed as a potential solution to harvest densification gain with reduced cost in terms of handover probability. In CP/UP split architecture, there is a control AP ($AP\ C$) in AS, which takes charge of CP as a local mobility anchor. We assume that the best AP in the AS is the $AP\ C$, for example, the AP with the largest backhaul capacity. A UE can receive data packets from all the APs in AS while being controlled via the $AP\ C$. In our proposed model, only handovers of $AP\ C$ are managed through mobility management entity (MME) in the core network if direct X2 interface is not available, while handover process of other APs in AS is controlled by the $AP\ C$.

B. PROPAGATION MODEL

A path-loss plus fading propagation model is assumed in this paper. At any time t, the received signal strength measured by a mobile UE u from the k-th AP is given by

$$\Gamma_{u,k} = Ph_k \left\| r_{u,k} \right\|^{-\alpha}, \tag{1}$$

where $r_{u,k}$ is the distance between the UE u and the k-th AP, $\alpha > 2$ is the path loss exponent, h_k is the multipath fading effect of the k-th AP modeled by a multiplicative channel gain. We assume that the fading channel follows a Rayleigh distribution with mean one [10], which implies that the channel gain h_k is exponentially distributed with mean one, hence $h \sim \exp\ (1)$. The PDF of h is $f\ (h) = e^{-h}$.

In our model, a new frequency reuse scheme is adopted, where the full bandwidth is exploited inside an AS, and then reused in another AS. On the one hand, the APs in the same AS transmit data packets on different frequencies, and they cooperate perfectly to mitigate the interference inside the AS. On the other hand, the bandwidth is then reused in another AS to serve different user. In other words, all the APs in its AS serve the typical UE with no interference, the signal from APs out of the AS are interference for the typical UE.

C. MULTI-CONNECTIVITY MOBILITY MODEL

We assume that the UE moves a distance v in a unit time at an arbitrary angle θ with respect to the direction of the furthest connection. The distances between the UE and the APs in its AS change due to the movement of UE. Thus, the AS would update its members via the $AP\ C$ through UE's movement, which is called a handover process.

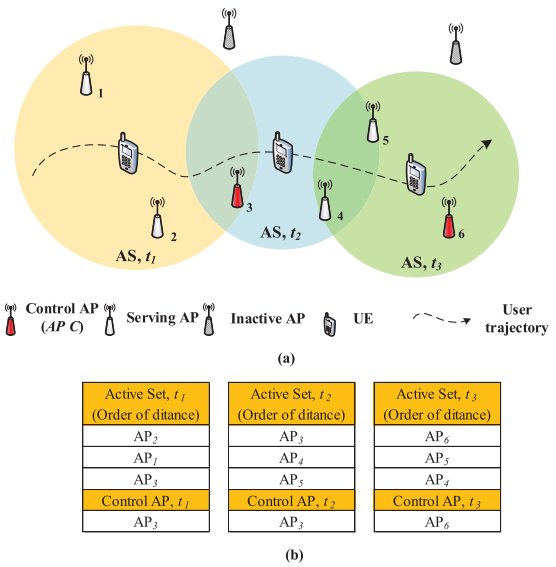

FIGURE 1. Multi-connectivity scenario where a UE connects with nearest three APs. UP handover occurs if the serving APs are changed (t_2); CP handover occurs if the serving control AP is leaving its active set (t_3).

In CP/UP split architecture, there is an $AP\ C$ in the AS serving as a local mobility anchor, showed in Fig. 1(a). The reference signal received power (RSRP) of APs in its vicinity are received and filtered by the UE through linear averaging, then reported to $AP\ C$. Hence, the filtered RSRP could be simplified to Received Signal Strength (RSS), which can be

expressed as

$$RSS_{u,k} = P\left\|r_{u,k}\right\|^{-\alpha}. \tag{2}$$

The handover decision process is based on RSS instead of RSRP to avoid unnecessary handover and ping-pong effect due to fast fading influences. Then, the *AP C* will decide whether adds a new AP to the AS while remove the farthest AP in the AS at the same time. In this case, the AS is always formed by the nearest M APs in user's neighborhood. Note that the add event always synchronize with the remove event, which terms as UP handover, defined the modification of any APs in AS. *AP C* will trigger UP handover if there is a new AP nearer than the furthest serving AP in the AS to make sure the AS is formed by the nearest M APs. Fig. 1(b) lists the tables of serving APs and *AP C* in the AS.

In order to guarantee there is always an *AP C* in the AS, the handover process in CP occurs when the serving *AP C* is leaving the AS according to the measurement report send from UE. When the serving *AP C* leaving its AS, the best AP among the AS is chosen to be the target *AP C*, taking over CP from the serving *AP C*. This process is termed as CP handover. Other APs in the AS remain transmitting data packets for the user during the handover process. It is significant to mention that UP handover process is managed by the *AP C*. The users would not be conscious of UP handover because the identities of the APs except the *AP C*s are hidden from the users. Only CP handovers would inform the MME in the core network.

III. HANDOVER PROBABILITY IN USER-PLANE

In our model, UE can receive data packets from the nearest M APs. For the purpose that the UE is in the center of its AS, the *AP C* have to decide UP handover event according to the measurement report. The UP handover probability is defined as the probability that UP handover occurs in a unit time. The notation H_u is used to denote UP handover event. Based on our system model, the UP handover probability $\mathrm{P}(H_u)$ can be calculated as

$$\begin{aligned}
&\mathrm{P}(H_u)\\
&= \sum_{j=1}^{M} \mathrm{P}\left(H_u|F_j\right)\mathrm{P}\left(F_j\right)\\
&= \frac{1}{\pi}\sum_{j=1}^{M}\iiint_{(V)} \mathrm{P}\left(H_u|F_j, r_{M+1}, r_j, \theta\right)\mathrm{P}\left(F_j|r_{M+1}, r_j, \theta\right)\\
&\quad \cdot f_{M+1|j}\left(r_{M+1}|r_j\right) f_j\left(r_j\right) dr_{M+1} dr_j d\theta.
\end{aligned} \tag{3}$$

where F_j denotes the event that *AP j* becomes the furthest serving AP after UE moved.

For the most part, we assume that the user can move in any direction with equal probability, and the probability of handover for the user moving at angle $(2\pi - \theta)$ is the same as that for the user moving at angle θ due to symmetry. Then, the probability distribution function (PDF) of θ is set to be a uniform distribution in $[0, \pi)$, that is $f_\theta(\theta) = 1/\pi$. $f_j(r)$ is the probability density function of the distance r to the j-th nearest small cell from the typical user at the origin which is given by [10]

$$f_j(r) = \frac{2}{\Gamma(j)}(\lambda_B \pi)^j r^{2j-1} e^{-\lambda_B \pi r^2}. \tag{4}$$

In order to solve the UP handover probability in (3), the conditional probability of UP handover $P(H_u|F_j, r_{M+1}, r_j, \theta)$, the conditional probability of being the furthest serving AP $\mathrm{P}(F_j|r_{M+1}, r_j, \theta)$, the conditional PDF of distance $f_{M+1|j}\left(r_{M+1}|r_j\right)$ and the integration domain are discussed later.

A. THE INTEGRATION DOMAIN

Based on the system model, when circle A is included in circle C, none of the new APs would present in circle A thus there must be no handover. In other words, handover occurs if and only if circle A intersects with circle C.

Lemma 1: According to our developed model, if and only if the relationship of the distances between UE and the serving *APs* r_j, r_{M+1} and the moving direction θ is in the following point set, it is possible that UP handover occurs:

$$(V) = (V_1) + (V_2) + (V_3), \tag{5}$$

where

$$(V_1) = \left\{ \left(r_j, r_{M+1}, \theta\right) \middle| \begin{array}{l} 0 < r_j < v, \\ r_j < r_{M+1} < 2v - r_j, \\ 0 < \theta < \pi \end{array} \right\},$$

$$(V_2) = \left\{ \left(r_j, r_{M+1}, \theta\right) \middle| \begin{array}{l} 0 < r_j < v, \\ 2v - r_j < r_{M+1} < 2v + r_j, \\ 0 < \theta < \cos^{-1}\left(\dfrac{r_{M+1}^2 - 2v r_{M+1} - r_j^2}{2 r_j v}\right) \end{array} \right\},$$

$$(V_3) = \left\{ \left(r_j, r_{M+1}, \theta\right) \middle| \begin{array}{l} r_j > v, \\ r_j < r_{M+1} < r_j + 2v, \\ 0 < \theta < \cos^{-1}\left(\dfrac{r_{M+1}^2 - 2v r_{M+1} - r_j^2}{2 r_j v}\right) \end{array} \right\}.$$

Proof: The proof is given in Appendix A. ■

Hence, the integration domain in (3) is limited by the above lemma.

B. THE CONDITIONAL PDF OF DISTANCE

The conditional probability density function of r_{M+1} is essential in the theoretical derivation. Similar to the analysis of $f_j(r)$ in [25], for $j < M$, the conditional cumulative distribution function (CDF) of r_M is the probability that there are less than $(M - j - 1)$ nodes closer than r_M conditioned on r_j.

Lemma 2: Consider a homogeneous network where the location of the APs follows a PPP with its density λ_B, let r_j and r_M be the distances between the UE and the serving APs where $j < M$. The probability density function of r_M

conditioned on r_j is given by

$$f_M\left(r_M|r_j\right) = 2r_M \frac{(\pi\lambda_B)^{M-j}}{\Gamma(M-j)}\left(r_M^2 - r_j^2\right)^{M-j-1} e^{-\lambda_B\pi\left(r_M^2-r_j^2\right)}, \tag{6}$$

where $\Gamma(\cdot)$ is the gamma function.

Proof: The proof is given in Appendix B. ■

Hence, from lemma 2, the conditional PDF $f_{M+1|j}\left(r_{M+1}|r_j\right)$ in (3) is given by

$$f_{M+1|j}\left(r_{M+1}|r_j\right) = 2r_{M+1} \frac{(\pi\lambda_B)^{M-j+1}}{\Gamma(M-j+1)}\left(r_{M+1}^2 - r_j^2\right)^{M-j} e^{-\lambda_B\pi\left(r_{M+1}^2-r_j^2\right)}. \tag{7}$$

C. THE CONDITIONAL PROBABILITY OF BEING THE FURTHEST AP

The furthest serving APs have to be found after UE moved since UP handover event is decided depending on the distance to the furthest AP and the distance to the nearest new AP. Therefore, *AP j* becomes the furthest serving AP only when no APs in the region $C\backslash A \cap C$. The region $C\backslash A \cap C$ need to split into two independent region: $S_I : C_j\backslash C_j \cap A$, and $S_{II} : (C\backslash A \cap C)\backslash S_I$. The region S_I is included by region C_j that contains $(j-1)$ APs; the region S_{II} is included by region $C\backslash C_j$ that contains $(M-j)$ APs. As the number of APs in circle C is a constant M, the APs in the aforementioned two independent part can be viewed as a conditional PPP, i.e. Binomial point process (BPP) [26]. The area of the two regions are

$$|S_I| = \pi r_j^2 - S_\cap\left(r_j, R, v\right), \tag{8}$$

and

$$\begin{aligned}|S_{II}| &= \pi r_{M+1}^2 - S_\cap(r_{M+1}, R, v) - S_I \\ &= \pi r_{M+1}^2 - \pi r_j^2 - S_\cap(r_{M+1}, R, v) + S_\cap\left(r_j, R, v\right),\end{aligned} \tag{9}$$

where $R^2 = r_j^2 + v^2 + 2vr_j\cos\theta$, $|S|$ is the area of the region S, the function $S_\cap(r, R, v)$ calculates the common area between two intersecting circles with radius r and R, where the central distance is v:

$$\begin{aligned}&S_\cap(r, R, v) \\ &= r^2\cos^{-1}\left(\frac{r^2+v^2-R^2}{2vr}\right) + R^2\cos^{-1}\left(\frac{R^2+v^2-r^2}{2vR}\right) \\ &\quad - \frac{1}{2}\sqrt{(r+R-v)(r+R+v)(v+r-R)(v-r+R)}.\end{aligned} \tag{10}$$

The area ratios of two BPPs are followed

$$\xi_I = \frac{|S_I|}{|C_j|} = \frac{\pi r_j^2 - S_\cap\left(r_j, R, v\right)}{\pi r_j^2}, \tag{11}$$

and

$$\begin{aligned}\xi_{II} &= \frac{|S_{II}|}{|C\backslash C_j|} \\ &= \frac{\pi r_{M+1}^2 - \pi r_j^2 - S_\cap(r_{M+1}, R, v) + S_\cap\left(r_j, R, v\right)}{\pi r_{M+1}^2 - \pi r_j^2}.\end{aligned} \tag{12}$$

According to the properties of BPP, the probability of the event F_j happened conditioned on r_j, r_{M+1} and θ is given by

$$\begin{aligned}P\left(F_j|r_{M+1}, r_j, \theta\right) &= P\left(N\left(|S_I|\right) = 0\right) P\left(N\left(|S_{II}|\right) = 0\right) \\ &= (1-\xi_I)^{j-1}(1-\xi_{II})^{M-j}.\end{aligned} \tag{13}$$

where $N(\cdot)$ denotes the number of APs in the specific area.

D. THE CONDITIONAL PROBABILITY OF HANDOVER IN USER-PLANE

It is possible that UP handover occurs when the *AP j* becomes the farthest serving AP in the AS after the UE moved. The conditional probability of UP handover not occur can be viewed as a product of two probabilities corresponding to independent events: (*a*) no APs remain in $A\backslash A \cap C$, (*b*) the *AP* $(M+1)$ is not located on the arc of circle C which is included in area A. For the purpose of simplicity, the notation N_{arc} is utilized to indicate the event *(b)*. Therefore, the expression of the conditional probability of UP handover is given by

$$\begin{aligned}&P\left(H_u|F_j, r_{M+1}, r_j, \theta\right) \\ &= 1 - P\left(\overline{H_u}|F_j, r_{M+1}, r_j, \theta\right) \\ &= 1 - P\left(N\left(|A\backslash A\cap C|\right) = 0\right) P\left(N_{arc}\right).\end{aligned} \tag{14}$$

According to the properties of PPP, the probability of finding n nodes in region S is given by the Poisson distribution

$$\mathrm{P}\left(N\left(|S|\right) = n\right) = \frac{\left(|S|\,\lambda_B\right)^n}{n!} e^{-|s|\lambda_B}. \tag{15}$$

When $n = 0$, $\mathrm{P}\left(N\left(|S|\right) = 0\right) = e^{-|s|\lambda_B}$. The area of $A\backslash A \cap C$ is given by

$$|A\backslash A \cap C| = \pi R^2 - S_\cap\left(r_{M+1}, R, v\right). \tag{16}$$

Insert (16) into (15) and set $n = 0$, the probability of event (*a*) can be solved.

The location of *AP* $(M+1)$ can be viewed as a one-dimensional uniformed distribution on the circle C. Hence the probability of complementary event of the event (*b*) is the ratio of length of the arc to the circumference of circle C. It is obvious that in plane geometry, the ratio can be transformed to the ratio of the corresponding central angle $\Delta\varphi$ and 2π. Thereby, the angle $\Delta\varphi$ satisfies the following equation

$$\cos\left(\frac{1}{2}\Delta\varphi\right) = \frac{r_{M+1}^2 - r_j^2 - 2vr_j\cos\theta}{2vr_{M+1}}. \tag{17}$$

The integration domain of the triple integral can guarantee the value range of $\frac{r_{M+1}^2 - r_j^2 - 2vr_j\cos\theta}{2vr_{M+1}}$ is between -1 and 1. Hence, from (17), the probability of $\mathrm{P}\left(N_{arc}\right)$ is obtained

$$\begin{aligned}P\left(N_{arc}\right) &= 1 - \frac{\Delta\varphi}{2\pi} \\ &= \frac{1}{\pi}\cos^{-1}\left(\frac{-r_{M+1}^2 + r_j^2 + 2vr_j\cos\theta}{2vr_{M+1}}\right).\end{aligned} \tag{18}$$

The probability of UP handover conditioned on F_j, r_j, r_{M+1} and θ is achieved by inserting (15), (16) and (18) into (14).

$$\mathrm{P}(H_u) = 4\pi\lambda_B^{M+1}\sum_{j=1}^{M}\frac{1}{\Gamma(M-j+1)\Gamma(j)}\iiint_{(V)} S_\cap\left(r_j,R,v\right)^{j-1}\left[S_\cap\left(r_{M+1},R,v\right)-S_\cap\left(r_j,R,v\right)\right]^{M-j}$$
$$\cdot\left[1-\frac{1}{\pi}\cos^{-1}\left(\frac{-r_{M+1}^2+r_j^2+2vr_j\cos\theta}{2vr_{M+1}}\right)e^{-\lambda_B\left(\pi R^2-S_\cap\left(r_{M+1},R,v\right)\right)}\right]e^{-\lambda_B\pi r_{M+1}^2}r_{M+1}r_j dr_{M+1}dr_j d\theta \quad (19)$$

So far, from (3), (4), (7), (13) and (14), the UP handover probability is given by (19), shown at the top of this page, where $R^2 = r_j^2 + v^2 + 2vr_j\cos\theta$, $\Gamma(\cdot)$ denotes the gamma function, the function $S_\cap(r,R,v)$ is given by (10), and the integration domain of the triple integral is given by (5).

IV. HANDOVER PROBABILITY IN CONTROL PLANE

The *AP C* controls the UE and takes charge of managing the radio resource control (RRC) procedures between UE and other APs in the AS serving for the UE, for example, it takes charge of session establishment and release. CP handover takes place when the serving *AP C* is away from the UE due to its movement. Hence, a target *AP C* is chosen and negotiates with the serving *AP C*. Similar to the theoretical analysis in section III, *AP* $(M+1)$ is taken into account for the sake of unity in analyses. Also, the PDF of θ_c is $f_{\theta_c}(\theta_c) = 1/\pi$ due to the symmetry. Different from the analysis in section III, whether the *AP C* becomes the furthest serving AP or not, CP handover process may occur. The CP handover probability can be calculated by

$$\begin{aligned}\mathrm{P}(H_c) &= \iiint_{(V_c)}\mathrm{P}(H_c|r_c,r_{M+1},\theta_c)f_{c|M+1,\theta_c}(r_c|r_{M+1},\theta_c)\\ &\quad\cdot f_{M+1|\theta_c}(r_{M+1}|\theta_c)f_{\theta_c}(\theta_c)\,dr_c dr_{M+1}d\theta_c\\ &= \frac{1}{\pi}\iiint_{(V_c)}\mathrm{P}(H_c|r_c,r_{M+1},\theta_c)f_{c|M+1}(r_c|r_{M+1})\\ &\quad\cdot f_{M+1}(r_{M+1})\,dr_c dr_{M+1}d\theta_c, \end{aligned}\quad (20)$$

where $f_{M+1}(r_{M+1})$ is the PDF of the distance r_{M+1} to the $(M+1)$-th nearest AP from the typical user at the origin given by (4). We assume that θ_c is independent of r_c and r_{M+1}, and the distribution of θ_c is uniform.

The multi-connectivity scheme can be transformed into single connectivity scheme when $M = 1$. In this case, only one AP connected with the UE transmits both control signal and data packets. This section assumes that at least two APs are serving the UE at the same time. According to lemma 1, by substituting r_c for r_{M+1}, substituting θ_c for θ, the integration domain (V_c) in calculation of CP handover probability in (20) can be obtained. The conditional CP handover probability $P(H_c|r_c,r_{M+1},\theta_c)$, and the conditional PDF of distance $f_{c|M+1}(r_c|r_{M+1})$ are discussed later.

A. THE CONDITIONAL PDF OF DISTANCE

The distance between the UE and the *AP C* in its AS is less than the distance between the UE and the *AP* $(M+1)$, hence the range of r_c is $(0, r_{M+1}]$. Since the AP with the largest backhaul capacity in the AS is chosen as *AP C* during the CP handover without considering its location, it is assumed that the distance between the UE and the *AP C* in its AS is random. In other words, the *AP C* follows a uniform distribution in the region C, which means the location of *AP C* follows a BPP. Therefore, the conditional CDF of r_c is

$$P(r_c \le r_{M+1}|r_{M+1}) = \frac{r_c^2}{r_{M+1}^2}, \quad (21)$$

and the conditional PDF of r_c is given by

$$f_{c|M+1}(r_c|r_{M+1}) = \frac{d}{dr}\frac{r_c^2}{r_{M+1}^2} = \frac{2r_c}{r_{M+1}^2}. \quad (22)$$

B. THE CONDITIONAL PROBABILITY OF HANDOVER CONTROL-PLANE

Different from UP handover, it is not necessary that *AP C* becomes the furthest serving AP after UE moved for triggering CP handover event. CP handover occurs when the number of AP in $C\backslash A_c \cap C$ is less than the number of APs in $A_c\backslash A_c \cap C$ and on its periphery. What's more, the number of APs in the region $C\backslash A_c \cap C$ could be arbitrary integer from zero to $(M-1)$. Comparing the number of APs in the two aforementioned region, the conditioned CP handover probability is given by the following theorem.

Theorem 1: Consider a multi-connectivity scenario where a mobile UE connects with nearest M APs in its vicinity and chooses the best one among them as the *AP C*. The locations of APs follows a PPP with its densityλ_B. r_c and r_{M+1} denote the distances between *AP C* or its $(M+1)$ nearest AP and the mobile UE, respectively. θ_c is the moving direction of UE to *AP C*. The CP handover probability conditioned on r_c, r_{M+1} and θ_c is given by

$$\begin{aligned}&P(H_c|r_c,r_{M+1},\theta_c)\\ &= 1-e^{-\left(\pi R_c^2-S_\cap(r_{M+1},R_c,v)\right)\lambda_B}\sum_{n=0}^{M-1}C_{M-1}^n\xi^n(1-\xi)^{M-n-1}\\ &\quad\cdot\sum_{k=0}^{n}P_n^k\frac{\left[\left(\pi R_c^2-S_\cap(r_{M+1},R_c,v)\right)\lambda_B\right]^k}{k!}, \end{aligned}\quad (23)$$

where $R_c = \sqrt{r_c^2+v^2+2vr_c\cos\theta_c}$, the $C_{M-1}^n = \frac{(M-1)!}{n!(M-n-1)!}$ is Binomial Coefficient, and the area ratio is denoted by $\xi = \frac{S_\cap(r_{M+1},R_c,v)}{\pi r_{M+1}^2}$, the function $S_\cap(\cdot,\cdot,\cdot)$ is given by (10), and

$$\mathrm{P}\left(H_c\right)=\frac{4\pi\lambda_B^{M+1}}{\Gamma\left(M+1\right)}\iiint_{(V_c)}\left[\left(\pi r_{M+1}^2\right)^{-M+1}-e^{-\lambda_B\left(\pi R_c^2-S_\cap\left(r_{M+1},R_c,v\right)\right)}\sum_{n=0}^{M-1}C_{M-1}^n\left(\pi r_{M+1}^2-S_\cap\left(r_{M+1},R_c,v\right)\right)^n\right.$$
$$\left.\cdot\left(S_\cap\left(r_{M+1},R_c,v\right)\right)^{M-n-1}\sum_{k=0}^{n}\frac{\left[\left(\pi R_c^2-S_\cap\left(r_{M+1},R_c,v\right)\right)\lambda_B\right]^k}{k!}\right]e^{-\lambda_B\pi r_{M+1}^2}r_{M+1}r_c dr_c dr_{M+1}d\theta_c \quad (24)$$

the coefficient P_n^k is given by

$$P_n^k=\begin{cases}1 & n\neq 0, k\neq n\\ \frac{1}{\pi}\cos^{-1}\left(\frac{-r_{M+1}^2+r_c^2+2vr_c\cos\theta_c}{2vr_{M+1}}\right) & n=0, or: n\neq 0,\quad k=n.\end{cases}$$

Proof: The proof is given in Appendix C. ■

Therefore, all the necessary values of CP handover probability are solved. Insert (4), (22) and (23) into (20), the expression of CP handover probability is derived in (24) shown at the top of this page.

V. MOBILITY-AWARE DOWNLINK RATE AND AREA SPECTRAL EFFICIENCY

In our system model, the UE connects to the nearest M APs in its vicinity. The average downlink rate $\bar{R}_j$ of the typical user while connected to the j-th AP in its AS is computed by Theorem 1 in [10]. Furthermore, the total downlink rate of a typical user without considering its mobility is the sum of $\bar{R}_j$, i.e.

$$R_M^s=\sum_{j=1}^{M}\bar{R}_j. \quad (25)$$

However, the expressions derived in [10] give the average downlink rate and area spectral efficiency without considering the user mobility as one of the main effects of network densification. In order to incorporate user mobility into our consideration, handover cost considering handover delays in both user-plane and control-plane are first analyzed. Taken advantage of the result of average downlink rate in [10], the mobility-aware downlink rate is finally derived in the subsection B.

A. HANDOVER COST

Handover cost is defined as the average duration consumed in handovers per unit time [17]. Hence, the handover cost considering handover probabilities in UP and CP can be expressed as:

$$D=\bar{d}_u\left[P\left(H_u\right)-P\left(H_c\right)\right]+\bar{d}_cP\left(H_c\right), \quad (26)$$

where $\bar{d}_u$ and $\bar{d}_c$ are the delays incurred by handover in UP and CP, respectively, $P\left(H_u\right)$ and $P\left(H_c\right)$ are the probabilities that handover occurs in UP and CP in a unit time, which are computed in section III and IV. It is important to note that when the control AP is leaving the AS, both UP handover and CP handover occur in our analysis. Here we assume that the probability that the user is experiencing a handover in UP without changing its $AP\ C$ is $[P\left(H_u\right)-P\left(H_c\right)]$.

In CP/UP split architecture, since the UP handovers are controlled by the $AP\ C$ in the AS without informing the core network, the handover delay incurred by UP handover is different from that incurred by CP handover. It is necessary to note that the core network elements are far away from the network edge usually and are mainly wired, which means the signaling overheads incurred by handovers in CP would transmit farther distances with lower speed. Therefore, the handover delay incurred by handover in UP is usually less than that incurred by handover in CP, i.e. $\bar{d}_u<\bar{d}_c$. Ibrahim *et al.* [17] take $\bar{d}_u=0.3\bar{d}_c$ and $\bar{d}_u=0.5\bar{d}_c$ as an example in numerical results.

What's more, it is significant to note that handover cost is a dimensionless unit, since the dimension of the delay and the handover rate are second/handover and handover/second, respectively. The handover delay is always less than 1 second, hence the handover cost in this paper is less than one. Therefore, the handover cost can also be seen as the probability that the typical user is experiencing a handover in a unit time.

B. MOBILITY-AWARE DOWNLINK RATE ANALYSIS

Incorporating the handover cost into the average downlink rate, we assume that the $AP\ j$ does not send data packets to the typical user while the other $(M-1)$ APs in the AS maintain their transmissions when the $AP\ j$ is leaving the AS [17]. Based on the assumption, the mobility-aware average downlink rate for CP/UP split multi-connectivity architecture can be expressed as

$$R_M=(1-D)\sum_{j=1}^{M}\bar{R}_j+D\sum_{j=1}^{M-1}\bar{R}_j, \quad (27)$$

where the first term the average downlink rate when handover in UP does not occur, while the second term is the average downlink rate when the typical user is experiencing the UP handover.

C. AREA SPECTRAL EFFICIENCY

The area spectral efficiency (ASE) is defined as the number of transmitted bits per second (bps) per Hz per unit area. ASE would be a significant performance metric in our user-centric association scenario. Since each user forms an AS by AP in its vicinity, the number of ASs is equal to that of users. Hence the user density multiplied by the accumulation of the average downlink rate in AS is ASE in multi-connectivity [10], which

is given by

$$ASE \triangleq \lambda_u R_M. \tag{28}$$

Since in UUDN the AP density is much larger than the user density, here we assume that each AP belongs to one AS, i.e. there is no overlapping between the ASs.

VI. NUMERICAL RESULTS

In this section, the analytical results are presented and are verified by simulations. (A) and (S) represent analytical and simulation results, respectively. The analytical results of UP handover probability, CP handover probability and downlink rate derived in Section III, IV and V, respectively, are calculated with typical value. We use one second as a unit time. Therefore, the moving distance can be seen as the UE velocity in the unit of meter/second (m/s). The numerical results present how the AP density λ_B, the velocity of UE v, the size of AS M have effects on handover probabilities and downlink rate of mobile users. Moreover, the handover probabilities for different the AS size M are exhibited to choose the most appropriate size M under different conditions. For mobility-aware downlink rate, it corresponds to the unit of nats/sec/Hz (1 nat/sec/Hz = 1.44 bps/Hz). As it is mentioned in [2], a quantitative measure of the density at which a network can be considered as ultra-dense networks is that small cell density more than or equal to 0.001 cells/m^2.

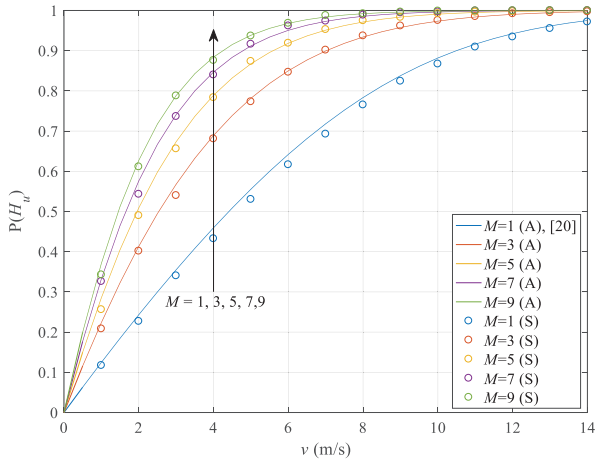

FIGURE 2. UP handover probability as a function of user velocity (AP density $\lambda_B = 0.01$ cells/m^2).

A. UP HANDOVER PROBABILITY

The UP handover probabilities as a function of user velocity are showed in Fig. 2 when the AP density is 0.01 cells/m^2. The simulations perfectly match the analytical results, validating the correctness of our analysis. The UP handover probability is almost proportional to the user velocity before the probability reaches 0.5. This is because that the number of UP handovers and UP handover probability in a unit time can be viewed as equal approximately and the closed-form expression of number of handovers in [24] also concludes that handover rate is proportional to the user velocity. It shows that the UP handover probabilities increase with the user velocity and it is obvious that with high velocity, the user will be far away from the serving APs after the movement, thus more likely to connect with new APs in the additional area. Compared with single connectivity, i.e. $M = 1$, the UP handover probability is higher for larger AS size. Although the UP handovers do not inform the core network, the handover signal overheads between APs and *AP C* cannot be ignored for large UP handover probability.

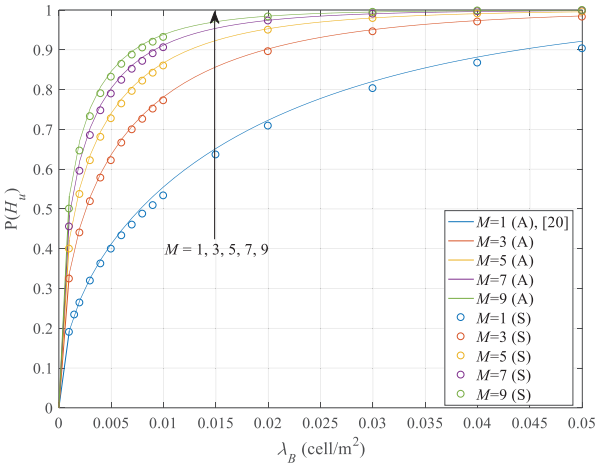

FIGURE 3. Effect of the AP density on UP handover probability (the user velocity is $v = 5$ m/s).

Fig. 3 shows the effect of the AP density on UP handover probabilities when the UE velocity is 5 m/s. The simulation results match our analysis as well. The UP handover probabilities increase sharply with the AP density from zero to 0.05 cells/m^2. The UP handover probability increases to 0.9 when AP density is 0.044, 0.020, 0.013, 0.009 and 0.007 cells/m^2 for AS size is 1, 3, 5, 7 and 9, respectively. It is consistent with our intuition that the probability converges to 1 at extremely large AP density, and the probability of larger AS size is higher. As the densification of AP deployment, the mobile UE is more likely to find a new AP nearer than the serving AP through the movement. Moreover, the AS updates its APs with higher probability for larger AS size, since the additional area is larger due to the user movement.

B. CP HANDOVER PROBABILITY

The CP handover probability as a function of user velocity is depicted in Fig. 4 when the AP density is 0.01 cells/m^2. Similar to Fig. 2, the CP handover probabilities increase with the user velocity. The probability of larger AS size is lower than that of smaller AS size, because the AS with larger AS size has large coverage, which decreases the probability for *AP C* leaving the AS. The CP handover probabilities reach to 0.9 when user velocity is 11, 17, 21, 25 and 28 m/s for $M = 1, 3, 5, 7$ and 9, respectively. The result shows that our multi-connectivity scheme decrease the handover probability for dense networks.

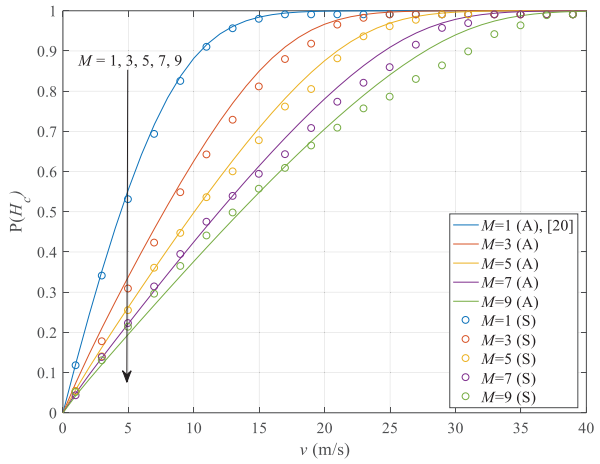

FIGURE 4. CP handover probability as a function of user velocity (AP density is $\lambda_B = 0.01$ cells/m^2).

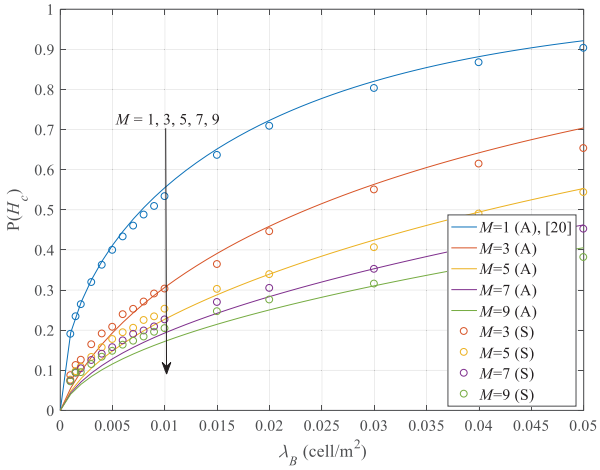

FIGURE 5. Effect of the AP density on CP handover probability (the user velocity is $v = 5$ m/s).

Fig. 5 illustrates the effect of the AP density on CP handover probability when the user velocity is 5 m/s. For $M = 1$, the UP handover probability (i.e. the blue curve in Fig. 2) and the CP handover probability (i.e. the blue curve in Fig. 5) stay the same. Although CP handover probability still goes up with the AP density, it decreases with larger AS size. When $\lambda_B = 0.05$ cells/m^2 and $v = 5$ m/s, the CP handover probabilities are 0.92, 0.70, 0.55, 0.46, 0.41 at $M = 1$, 3, 5, 7, 9, respectively. The decreases diminish with AS size.

Computer simulation is conducted to validate the correctness of our analysis. As we can see in Figs. 4 and 5, the simulation and analytical results mismatch each other for cases with large AS size. This is because when the AS size is large, the assumption that the *AP C* is the AP with largest backhaul capacity in the AS and thus follows a uniform distribution does not always hold, since there is a slight chance that the AP with a larger backhaul capacity is added into the AS. However, the probability of adding an AP with larger backhaul capacity is small intuitively and the simulation results shows the difference can be ignored.

Compare to the UP handover probability in Fig. 3, the difference between two handover probabilities is growing with larger AS size. For example, when $M = 3$ and $\lambda_B = 0.02$ cells/m^2, the probability shrinks from 0.90 to 0.46; the curves that $M = 5$ is from 0.95 to 0.34; the curves that $M = 7$ is from 0.97 to 0.28; and the decrease is from 0.98 to 0.25 when $M = 9$. The decrease is 48.9%, 64.2%, 71%, 74%, respectively. Quantitatively, although the CP handover probability decrease is expanding, the gain of the decrease is shirking.

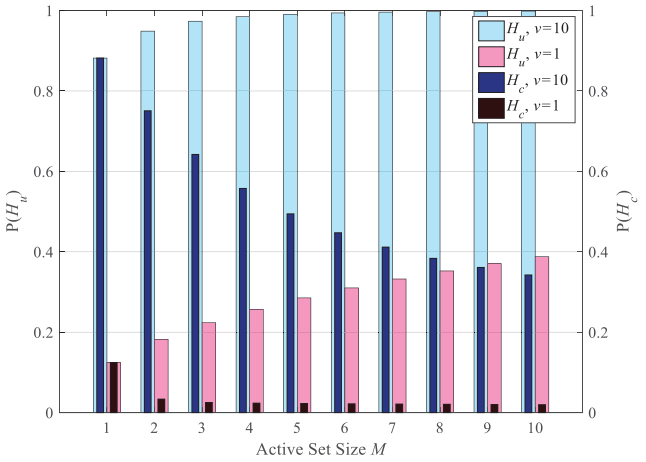

FIGURE 6. Relationship between active set size M and handover probabilities in both control-plane and user-plane (AP density λ_B is 0.01 cells/m^2).

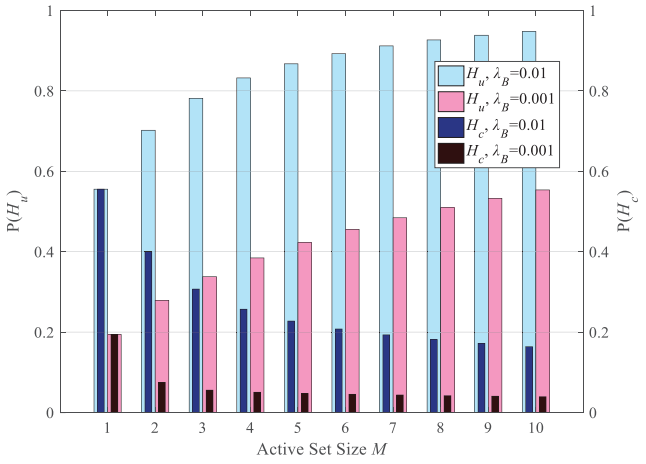

FIGURE 7. Relationship between active set size M and handover probabilities in both control-plane and user-plane (UE velocity v is 5 m/s).

C. AS SIZE AND HANDOVER PROBABILITIES

Figs. 6 and 7 illustrate the differences between the UP handover probability and the CP handover probability versus AS sizes for different user velocities or AP density. We take user velocity $v = 1$ m/s and $v = 10$ m/s, which are the typical walking velocity and low vehicle speed on urban roadways, respectively, while AP density $\lambda_B = 0.001$ cells/m^2, which is the boundary between UUDN and traditional networks,

and $\lambda_B = 0.01$ cells/m^2, as an example. It is important to note that UP handover under our CP/UP split architecture is equal to handover in traditional cellular system where all the handovers are managed through MME if direct X2 interface between the serving and the target APs is not available. Hence, the differences between UP handover probability (the bars with light color) and CP handover probability (the bars with dark color) are the gains brought by the proposed CP/UP split UUDN architecture.

The increase of UP handover probability can be seen as the cost of larger AS size. Since the AS size is X-axis, the decrease brought by the larger size can be observed visually. For an arbitrary given AP density and user velocity, the difference between two probabilities increases at first, but tends to be flat finally. Therefore, there is a corresponding optimal size for different AP density and user velocity to compromise the two probabilities. For example, when $\lambda_B = 0.01$ cells/m^2 and $v = 1$ m/s in Fig. 6, the optimal size is 2 since the CP handover probability decrease slightly when the size is more than 2; while, when $\lambda_B = 0.01$ cells/m^2 and $v = 5$ m/s in Fig. 7, the optimal size will be 5.

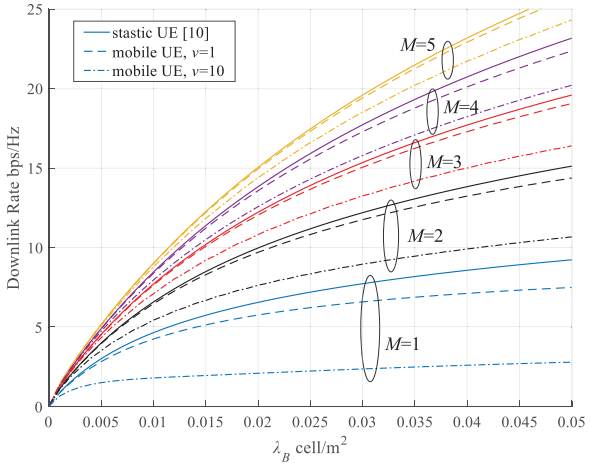

FIGURE 8. Average downlink rate versus AP density for different AS size and user mobility ($\bar{d}_C = 0.7$s, $\bar{d}_U = 0.3$s).

D. MOBILITY-AWARE DOWNLINK RATE

Fig. 8 shows the average downlink rate per user versus different AS size and user mobility. The results show that the average downlink rate increases with higher AP density. Moreover, user's downlink rate with larger AS size M is always higher than that with smaller AS size. The mobile users' downlink rates are lower than static users' downlink rates since mobile user would experience handover. Furthermore, the average downlink rate decreases with user's velocity. It is obvious that users with high mobility would suffer from more handovers and thus experience lower downlink rate.

E. AREA SPECTRAL EFFICIENCY

Fig. 9 illustrates the area spectral efficiency versus user density for different AS size and user mobility. In our analysis,

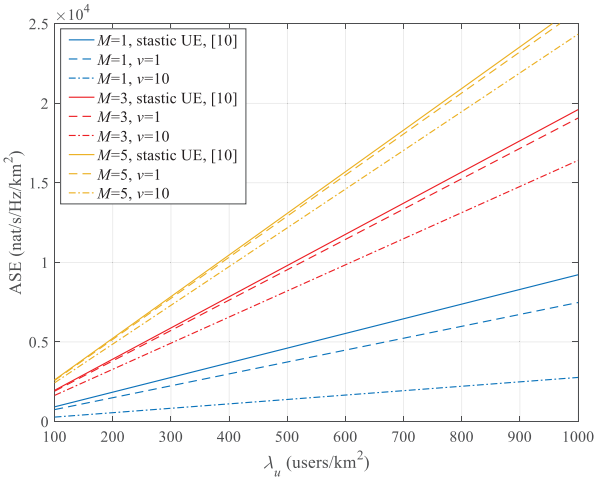

FIGURE 9. Area spectral efficiency versus user density for different AS size and user mobility ($\lambda_B = 0.05$, $\bar{d}_C = 0.7$s, $\bar{d}_U = 0.3$s).

area spectral efficiency is the cumulate downlink rate multiplied by user density. Hence, the ASE increases linearly with user density. The ASE with larger AS size is higher than that with smaller AS size accordingly. On the other hand, the gains are diminishing with AS size. The effect of user mobility can also be seen in Fig. 9. Similarly, the users with higher mobility would decrease the ASE.

VII. CONCLUSION

In order to enhance mobility performance for mobile users in dense networks, this paper proposes a multi-connectivity scheme with CP/UP split architecture in 5G UUDN environment. By making it possible to maintain connections with more than one APs, a UE can enjoy continuous service when one or more APs are leaving its AS. Handover probabilities are first derived, and by including handover probabilities into handover cost, the average downlink rate of mobile users is obtained. In UUDN with CP/UP split architecture, handover probabilities achieve a decrease of more than 50% compared with traditional networks. Moreover, we propose that there will be a corresponding optimal AS size for different condition to compromise sharply increased UP handover probability and CP handover probability managed by MME. The average downlink rate increases significantly in the multi-connectivity mobility model as well.

For further study, the performance of multi-connectivity scheme can be studied on different cell selecting mechanism and cooperation scheme. It is significant to mention that multi-connectivity mobility for UUDN has not been investigated in stochastic geometry before, and it would be a revolutionary mark.

APPENDICES

A. PROOF OF LEMMA 1

Only when circle A intersects circle C after the user moving a distance v, there would be a chance that UP handover occurs.

According to plane geometry, the condition that the two circle intersect with each other is given by

$$\begin{aligned} A \cap C &\Leftrightarrow |r_{M+1} - R| < v < r_{M+1} + R \\ &\Leftrightarrow (r_{M+1} - v)^2 < R^2 < (r_{M+1} + v)^2 \\ &\Leftrightarrow r_{M+1}^2 - 2vr_{M+1} < r_j^2 + 2vr_j \cos\theta \\ &\Leftrightarrow \cos\theta > \delta, \end{aligned} \tag{29}$$

where $\delta \triangleq \frac{r_{M+1}^2 - 2vr_{M+1} - r_j^2}{2vr_j}$.

For $\delta < -1$, i.e. $r_{M+1} + r_j < 2v$, the inequality (29) must hold; on the other hand, for $\delta > 1$, i.e. $r_{M+1} - r_j > 2v$, the inequality (29) cannot hold. While, when $-1 < \delta < 1$, the range of θ have to narrow down to $\left[0, \cos^{-1}\left(\frac{r_{M+1}^2 - 2vr_{M+1} - r_j^2}{2vr_j}\right)\right)$ to meet (29). Therefore, the integration domain is narrowed down to (5). Proof is completed.

B. PROOF OF LEMMA 2

The CDF of r_M conditioned on r_j is given by

$$\begin{aligned} &P\left(N\left(\left|C_M/C_j\right|\right) \le M - j - 1\right) \\ &= \sum_{k=0}^{M-j-1} P\left(N\left(\left|C_M/C_j\right|\right) = k\right) \\ &= \sum_{k=0}^{M-j-1} \frac{\left[\left(\pi r_M^2 - \pi r_j^2\right)\lambda_B\right]^k}{k!} e^{-\lambda_B\left(\pi r_M^2 - \pi r_j^2\right)}. \end{aligned} \tag{30}$$

Based on (30), the PDF of r_M is given by

$$\begin{aligned} &f_{M|j}\left(r_M|r_j\right) \\ &= \frac{d}{dr_M}\left[1 - P\left(N\left(\left|C_M/C_j\right|\right) \le M - j - 1\right)\right] \\ &= -\frac{d}{dr_M} P\left(N\left(\left|C_M/C_j\right|\right) \le M - j - 1\right) \\ &= -\frac{d}{dr_M} \sum_{k=0}^{M-j-1} P\left(N\left(\left|C_M/C_j\right|\right) = k\right) \\ &= \sum_{k=0}^{M-j-1} \left[-\frac{d}{dr_M} P\left(N\left(\left|C_M/C_j\right|\right) = k\right)\right]. \end{aligned} \tag{31}$$

For $k \ge 1$,

$$\begin{aligned} &\frac{d}{dr_M} P\left(N\left(\left|C_M/C_j\right|\right) = k\right) \\ &= 2r_M k\left(r_M^2 - r_j^2\right)^{k-1} \frac{(\pi\lambda_B)^k}{k!} e^{-\lambda_B\pi\left(r_M^2 - r_j^2\right)} \\ &\quad - 2r_M \pi\lambda_B \left(r_M^2 - r_j^2\right)^k \frac{(\pi\lambda_B)^k}{k!} e^{-\lambda_B\pi\left(r_M^2 - r_j^2\right)} \\ &= 2r_M \left[\frac{(\pi\lambda_B)^k}{(k-1)!}\left(r_M^2 - r_j^2\right)^{k-1} - \frac{(\pi\lambda_B)^{k+1}}{k!}\left(r_M^2 - r_j^2\right)^k\right] \\ &\quad \cdot e^{-\lambda_B\pi\left(r_M^2 - r_j^2\right)} \\ &\triangleq 2r_M \left(S_{k-1} - S_k\right) e^{-\lambda_B\pi\left(r_M^2 - r_j^2\right)}, \end{aligned} \tag{32}$$

where $S_k = \frac{(\pi\lambda_B)^{k+1}}{k!}\left(r_M^2 - r_j^2\right)^k$ for the sake of simplicity.

For $k = 0$, i.e. $P\left(N\left(\left|C_M/C_j\right|\right) = 0\right) = e^{-\lambda_B\pi\left(r_M^2 - r_j^2\right)}$, then

$$\begin{aligned} &\frac{d}{dr_M} P\left(N\left(\left|C_M/C_j\right|\right) = 0\right) \\ &= -2r_M \lambda_B \pi e^{-\lambda_B\pi\left(r_M^2 - r_j^2\right)} \\ &= -2r_M S_0 e^{-\lambda_B\pi\left(r_M^2 - r_j^2\right)}. \end{aligned} \tag{33}$$

From (30) - (33), we have

$$\begin{aligned} &f_M\left(r_M|r_j\right) \\ &= \sum_{k=0}^{M-j-1} \left[-\frac{d}{dr_M} P\left(N\left(\left|C_M/C_j\right|\right) = k\right)\right] \\ &= \sum_{k=1}^{M-j-1} 2r_M \left(S_k - S_{k-1}\right) e^{-\lambda_B\pi\left(r_M^2 - r_j^2\right)} \\ &\quad + 2r_M S_0 e^{-\lambda_B\pi\left(r_M^2 - r_j^2\right)} \\ &= 2r_M \left(\sum_{k=0}^{M-j-1} S_k - \sum_{k=0}^{M-j-2} S_k\right) e^{-\lambda_B\pi\left(r_M^2 - r_j^2\right)} \\ &= 2r_M S_{M-j-1} e^{-\lambda_B\pi\left(r_M^2 - r_j^2\right)} \\ &= 2r_M \frac{(\pi\lambda_B)^{M-j}}{\Gamma(M-j)}\left(r_M^2 - r_j^2\right)^{M-j-1} e^{-\lambda_B\pi\left(r_M^2 - r_j^2\right)}. \end{aligned} \tag{34}$$

The proof is completed.

C. PROOF OF THEOREM 1

Let N_{arc}^c denotes the event that the arc of circle C which is included in area A_c have to be exclusive of AP. Then, the conditional probability of not-handover could be expressed by (35), shown at the top of the next page.

In plane geometry, the $P\left(\bar{N}_{arc}^c\right)$ is the ratio between the arc of circle C which is included in area A and the perimeter of circle C, which is equal to the ratio between the central angle of the arc $\Delta\varphi$ and 2π. As same as the analysis of N_{arc} and the expression of $P\left(N_{arc}\right)$ in (18), let r_c substitutes r_j, θ_c substitutes θ, and the expression of $P\left(N_{arc}^c\right)$ is given by

$$P\left(N_{arc}^c\right) = \frac{1}{\pi}\cos^{-1}\left(\frac{-r_{M+1}^2 + r_c^2 + 2vr_c\cos\theta_c}{2vr_{M+1}}\right). \tag{36}$$

The number of APs in the region $A_c \backslash A_c \cap C$ follows a PPP. According to (15) and the area of $A_c \backslash A_c \cap C$ which is $\pi R_c^2 - S_\cap\left(r_{M+1}, R_c, v\right)$, the probability of finding n APs in $A_c \backslash A_c \cap C$ is given by

$$\begin{aligned} &P\left(N\left(\left|A_c \backslash A_c \cap C\right|\right) = n\right) \\ &= \frac{\left[\left(\pi R_c^2 - S_\cap\left(r_{M+1}, R_c, v\right)\right)\lambda_B\right]^n}{n!} e^{-\left(\pi R_c^2 - S_\cap\left(r_{M+1}, R_c, v\right)\right)\lambda_B}. \end{aligned} \tag{37}$$

On the other hand, the number of APs in the region $C \backslash A_c \cap C$ whose area is $\pi r_{M+1}^2 - S_\cap\left(r_{M+1}, R_c, v\right)$ follows

$$
\begin{aligned}
&P\left(\bar{H}_c|r_c, r_{M+1}, \theta_c\right) \\
&= P\left(N^c_{arc}\right) P\left(N\left(|A_c \backslash A_c \cap C|\right) \leq N\left(|C \backslash A_c \cap C|\right)\right) + P\left(\bar{N}^c_{arc}\right) P\left(N\left(|A_c \backslash A_c \cap C|\right) \leq N\left(|C \backslash A_c \cap C|\right) - 1\right) \\
&= \sum_{n=1}^{M-1} P\left(N\left(|C \backslash A_c \cap C|\right) = n\right) \sum_{k=0}^{n-1} P\left(N\left(|A_c \backslash A_c \cap C|\right) = k\right) \\
&\quad + \sum_{n=0}^{M-1} P\left(N\left(|C \backslash A_c \cap C|\right) = n\right) P\left(N^c_{arc}\right) \cdot P\left(N\left(|A_c \backslash A_c \cap C|\right) = n\right)
\end{aligned} \tag{35}
$$

a BPP. According to the properties of BPP, the probability of finding n nodes in the region is given by

$$
\begin{aligned}
&P\left(N\left(|C \backslash A \cap C|\right) = n\right) \\
&= C^n_{M-1} \left(\frac{\pi r^2_{M+1} - S_{\cap}\left(r_{M+1}, R_c, v\right)}{\pi r^2_{M+1}} \right)^n \\
&\quad \times \left(\frac{S_{\cap}\left(r_{M+1}, R_c, v\right)}{\pi r^2_{M+1}} \right)^{M-n-1},
\end{aligned} \tag{38}
$$

where $C^n_{M-1} = \frac{(M-1)!}{n!(M-n-1)!}$ is Binomial Coefficient.

In order to combine the two term in the last step in (35), a coefficient P^k_n is introduced as a substitute of the effect of $\sum_{k=0}^{n-1} P\left(N\left(|A_c \backslash A_c \cap C|\right) = k\right)$ and $P\left(N^c_{arc}\right)$. Thus, P_n is given by

$$
P^k_n = \begin{cases} P\left(N^c_{arc}\right) & n = 0, or: n \neq 0, k = n \\ 1 & n \neq 0, k \neq n. \end{cases} \tag{39}
$$

From (35)-(39), and the complementary relation of H and $\bar{H}$ $P\left(H|r_c, r_{M+1}, \theta_c\right) = 1 - P\left(\bar{H}|r_c, r_{M+1}, \theta_c\right)$, we can derive the result in (24) and complete the proof.

REFERENCES

[1] Y. Gu, Q. Cui, Y. Chen, W. Ni, X. Tao, and P. Zhang, "Effective capacity analysis in ultra-dense wireless networks with random interference," *IEEE Access*, vol. 6, pp. 19499–19508, Mar. 2018.

[2] M. Kamel, W. Hamouda, and A. Youssef, "Ultra-dense networks: A survey," *IEEE Commun. Surveys Tuts.*, vol. 18, no. 4, pp. 2522–2545, 4th Quart., 2016.

[3] H. Zhang, Y. Chen, Z. Yang, and X. Zhang, "Flexible coverage for Backhaul-limited ultradense heterogeneous networks: Throughput analysis and η-optimal biasing," *IEEE Trans. Veh. Technol.*, vol. 67, no. 5, pp. 4161–4172, May 2018.

[4] D. Calabuig *et al.*, "Resource and mobility management in the network layer of 5G cellular ultra-dense networks," *IEEE Commun. Mag.*, vol. 55, no. 6, pp. 162–169, Jun. 2017.

[5] S. Chen, F. Qin, B. Hu, X. Li, and Z. Chen, "User-centric ultra-dense networks for 5G: Challenges, methodologies, and directions," *IEEE Wireless Commun.*, vol. 23, no. 2, pp. 78–85, Apr. 2016.

[6] H. Zhang, Z. Yang, Y. Liu, and X. Zhang, "Power control for 5G user-centric network: Performance analysis and design insight," *IEEE Access*, vol. 4, pp. 7347–7355, Oct. 2016.

[7] H. Zhang, N. Meng, Y. Liu, and X. Zhang, "Performance evaluation for local anchor-based dual connectivity in 5G user-centric network," *IEEE Access*, vol. 4, pp. 5721–5729, 2016.

[8] F. B. Tesema, A. Awada, I. Viering, M. Simsek, and G. Fettweis, "Evaluation of context-aware mobility robustness optimization and multi-connectivity in intra-frequency 5G ultra dense networks," *IEEE Wireless Commun. Lett.*, vol. 5, no. 6, pp. 608–611, Dec. 2016.

[9] S. Chandrashekar, A. Maeder, C. Sartori, T. Höhne, B. Vejlgaard, and D. Chandramouli, "5G multi-RAT multi-connectivity architecture," in *Proc. IEEE Int. Conf. Commun. Workshops (ICC)*, Kuala Lumpur, Malaysia, May 2016, pp. 180–186.

[10] M. I. Kamel, W. Hamouda, and A. M. Youssef, "Multiple association in ultra-dense networks," in *Proc. IEEE Int. Conf. Commun. Workshops (ICC)*, Kuala Lumpur, Malaysia, May 2016, pp. 1–6.

[11] M. Kamel, W. Hamouda, and A. Youssef, "Performance analysis of multiple association in ultra-dense networks," *IEEE Trans. Commun.*, vol. 65, no. 9, pp. 3818–3831, Sep. 2017.

[12] F. B. Tesema, A. Awada, I. Viering, M. Simsek, and G. P. Fettweis, "Mobility modeling and performance evaluation of multi-connectivity in 5G intra-frequency networks," in *Proc. IEEE Globecom Workshops (GC Wkshps)*, San Diego, CA, USA, Dec. 2015, pp. 1–6.

[13] C. Rosa *et al.*, "Dual connectivity for LTE small cell evolution: Functionality and performance aspects," *IEEE Commun. Mag.*, vol. 54, no. 6, pp. 137–143, Jun. 2016.

[14] V. Petrov *et al.*, "Dynamic multi-connectivity performance in ultra-dense urban mmWave deployments," *IEEE J. Sel. Areas Commun.*, vol. 35, no. 9, pp. 2038–2055, Sep. 2017.

[15] M. Polese, M. Giordani, M. Mezzavilla, S. Rangan, and M. Zorzi, "Improved handover through dual connectivity in 5G mmWave mobile networks," *IEEE J. Sel. Areas Commun.*, vol. 35, no. 9, pp. 2069–2084, Sep. 2017.

[16] W. Bao and B. Liang, "Optimizing cluster size through handoff analysis in user-centric cooperative wireless networks," *IEEE Trans. Wireless Commun.*, vol. 17, no. 2, pp. 766–778, Feb. 2018.

[17] H. Ibrahim, H. ElSawy, U. T. Nguyen, and M. S. Alouini, "Mobility-aware modeling and analysis of dense cellular networks with C-plane/U-plane split architecture," *IEEE Trans. Commun.*, vol. 64, no. 11, pp. 4879–4894, Nov. 2016.

[18] X. Lin, R. K. Ganti, P. J. Fleming, and J. G. Andrews, "Towards understanding the fundamentals of mobility in cellular networks," *IEEE Trans. Wireless Commun.*, vol. 12, no. 4, pp. 1686–1698, Apr. 2013.

[19] F. Guidolin, I. Pappalardo, A. Zanella, and M. Zorzi, "Context-aware handover policies in HetNets," *IEEE Trans. Wireless Commun.*, vol. 15, no. 3, pp. 1895–1906, Mar. 2016.

[20] S. Sadr and R. S. Adve, "Handoff rate and coverage analysis in multi-tier heterogeneous networks," *IEEE Trans. Wireless Commun.*, vol. 14, no. 5, pp. 2626–2638, May 2015.

[21] W. Bao and B. Liang, "Stochastic geometric analysis of user mobility in heterogeneous wireless networks," *IEEE J. Sel. Areas Commun.*, vol. 33, no. 10, pp. 2212–2225, Oct. 2015.

[22] S.-Y. Hsueh and K.-H. Liu, "An equivalent analysis for handoff probability in heterogeneous cellular networks," *IEEE Commun. Lett.*, vol. 21, no. 6, pp. 1405–1408, Jun. 2017.

[23] Y. Teng, M. Liu, and M. Song, "Effect of outdated CSI on handover decisions in dense networks," *IEEE Commun. Lett.*, vol. 21, no. 10, pp. 2238–2241, Oct. 2017.

[24] W. Bao and B. Liang, "Stochastic geometric analysis of handoffs in user-centric cooperative wireless networks," in *Proc. IEEE Int. Conf. Comput. Commun. (ICCC)*, San Francisco, CA, USA, Apr. 2016, pp. 1–9.

[25] M. Haenggi, "On distances in uniformly random networks," *IEEE Trans. Inf. Theory*, vol. 51, no. 10, pp. 3584–3586, Oct. 2005.

[26] M. Haenggi, *Stochastic Geometry for Wireless Networks*. Cambridge, U.K.: Cambridge Univ. Press, 2012.

HONGTAO ZHANG received the Ph.D. degree in communication and information systems from the Beijing University of Posts and Telecommunications (BUPT), China, in 2008. He is currently an Associate Professor with the School of Information and Communications Engineering, BUPT. He has published over 60 articles in international journals and conferences. He held over 30 patents. He is the author of seven technical books. His research interests include 5G wireless communication and signal processing.

WANQING HUANG received the bachelor's degree in communication engineering from the Beijing University of Posts and Telecommunications (BUPT) in 2017, where she is currently pursuing the M. Tech. degree in communication and information engineering with the School of Information and Communication Engineering. Her research interest includes the emerging technologies of 5G wireless communication networks.